

Analysis of PZT Piezoelectric Sensors in Buckling Mode for Dynamic Strain Measurement

Ghaderiaram, Aliakbar; Schlangen, Erik; Fotouhi, Mohammad

DOI

[10.58286/29596](https://doi.org/10.58286/29596)

Publication date

2024

Document Version

Final published version

Published in

e-Journal of Nondestructive Testing

Citation (APA)

Ghaderiaram, A., Schlangen, E., & Fotouhi, M. (2024). Analysis of PZT Piezoelectric Sensors in Buckling Mode for Dynamic Strain Measurement. *e-Journal of Nondestructive Testing*, 1-8.
<https://doi.org/10.58286/29596>

Important note

To cite this publication, please use the final published version (if applicable).
Please check the document version above.

Copyright

Other than for strictly personal use, it is not permitted to download, forward or distribute the text or part of it, without the consent of the author(s) and/or copyright holder(s), unless the work is under an open content license such as Creative Commons.

Takedown policy

Please contact us and provide details if you believe this document breaches copyrights.
We will remove access to the work immediately and investigate your claim.

Analysis of PZT Piezoelectric Sensors in Buckling Mode for Dynamic Strain Measurement

Aliakbar GHADERIARAM¹, Erik SCHLANGEN², Mohammad FOTOUHI³

¹The Delft University of Technology, Delft, Netherlands, a.ghaderiaram@tudelft.nl

²The Delft University of Technology, Delft, Netherlands, erik.schlangen@tudelft.nl

³The Delft University of Technology, Delft, Netherlands, m.fotouhi-1@tudelft.nl

Abstract. Fatigue Life Monitoring is crucial to ensuring the safety and durability of engineering structures. This paper presents an innovative approach for fatigue life monitoring using a PZT (Lead Zirconate Titanate) piezoelectric sensor operating in buckling mode to measure applied cyclic strains. A significant focus is placed on the utilization of a 3D-printed 'Extension' platform upon which the PZT sensor is installed, allowing it to operate in buckling mode while subjected to cyclic strains. An analytical framework is developed to establish a direct relationship between dynamic strain values and the sensor's output, considering critical strain attributes such as amplitude and strain rate. The analytical solutions are validated through a series of experimental tests conducted under various dynamic loading conditions. Integrating the piezoelectric sensor with the 3D-printed extension demonstrates high sensitivity and serves as a passive dynamic strain measurement sensor, with promising potential for application as sensor nodes in fatigue life monitoring of engineering structures.

Keywords: Fatigue life, Piezoelectric sensor, Buckling mode, Dynamic strain

Introduction

The structural integrity and performance of engineering components and materials are critical considerations in ensuring the safety and reliability of various systems. One pivotal aspect of this assessment is the monitoring of fatigue life, particularly in dynamic environments where materials are subjected to cyclic loading [1]. Fatigue failure, often characterized by the progressive development of cracks, is a prevalent concern in engineering structures, ranging from bridges and aircraft to electronic devices [2]. Accurate and timely measurement of strain cycles can be used as a proactive assessment method for the evaluation of potential fatigue failure.

The selection of suitable sensors stands as a critical decision in ensuring accurate and comprehensive data acquisition of dynamic strains. Various sensor types have been employed to capture the dynamic strain behaviour inherent in cyclic loading scenarios. Each



sensor type brings unique advantages and limitations. Strain gauges, commonly used for static strain measurements, face limitations in the high-frequency domain, making them less suitable in capturing rapid cyclic changes. Accelerometers, designed to measure acceleration, provide insights into dynamic loading but may not directly measure strain [3]. Fibre optic sensors, known for their versatility, exhibit promise in some applications but may face challenges like limited angles, temperature variation and pH condition in certain environmental conditions[4].

Due to high sensitivity, piezoelectric sensors emerge as a versatile and effective choice for dynamic strain measurement among a variety of sensors [5]. These sensors operate on the principle of converting mechanical deformation into electrical charge, allowing them to capture rapid and subtle changes in strain. Different types of piezoelectric sensors are tailored for specific applications, including lead zirconate titanate (PZT), quartz, and polyvinylidene fluoride (PVDF) sensors [6]. Notably, PZT sensors exhibit exceptional sensitivity and stability, making them well-suited for dynamic applications [7]. In addition to functioning as strain gauges, certain piezoelectric sensors can serve as ultrasonic transducers, enabling the detection of ultrasonic waves and providing insights into material properties and degradation mechanisms. Moreover, their capability to capture acoustic emission, linked to the release of transient stress waves during active cracks and damage, further enhances their utility in monitoring the health and integrity of structures[5].

Sirohi et al. [8] investigated piezoelectric elements (PZT and PVDF) as strain sensors, comparing them with conventional foil strain gages. Surface-bonded to a beam, the sensors were calibrated, addressing transverse strain and shear lag effects. Temperature effects on PZT sensors were examined, and superior sensitivity and signal-to-noise ratio demonstrated the advantages of piezoelectric sensors over conventional counterparts. In another study, piezoelectric was used as a strain gauge in buckling mode[7], and the performance was evaluated analytically and experimentally under mechanical loads [9], [10]. In a recent study, cyclic strains was measured using a PZT in buckling mode. A 3D-printed extension part was developed and affixed to structures with epoxy glue. This extension converts structural strain to PZT's bending chord, preventing sensor rupture in high-strain scenarios and enabling one-dimensional strain measurement. Preliminary results demonstrate the extension's functionality, showing a linear increase in the PZT's output with tensile strain, consistent with the piezoelectric governing Equation [7].

This article investigates the behaviour of a piezoelectric sensor in buckling mode and aims to provide analytical modelling for measuring cyclic strains. The buckling mode was created using the extension part [7] that converts structural strain into PZT's bending chord, preventing sensor rupture in highly strained scenarios, and facilitating precise one-dimensional strain measurement.

1. Methodology

1.1 Piezoelectricity

Piezoelectric materials generate an electric charge in response to mechanical stress or deformation[6]. Fig. 1 shows the simplified configuration of a quartz crystal, showcasing its diverse states. In its pristine state, the positive charge center (C_{Q+}) aligns precisely with the negative charge center (C_{Q-}), ensuring external electrical neutrality. Yet, under mechanical deformations, these charge centres diverge, prompting the emergence of electric dipole moments from C_{Q-} to C_{Q+} . This polarization, denoted as P , intensifies with the geometric separation between C_{Q-} and C_{Q+} . Upon short-circuiting the electrodes, a consequential charge flow, or electric current, ensues. Alternatively, electrically unloading the electrodes

facilitates the measurement of an electric voltage across them, providing a nuanced glimpse into the intricate interplay of electrical and mechanical phenomena within the realm of piezoelectricity.

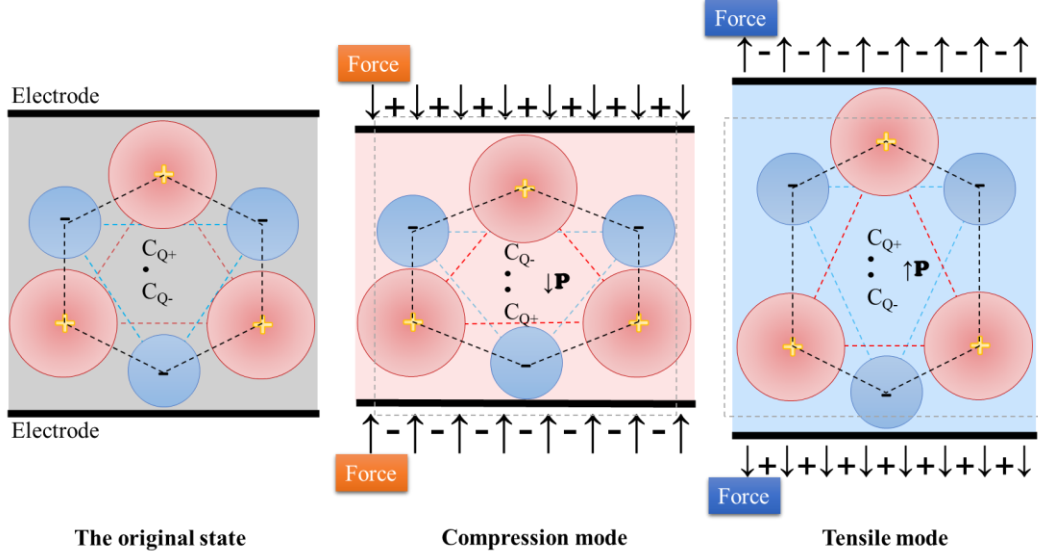


Fig. 1. Schematic depicting the internal structure of a quartz crystal flanked by electrodes on two surfaces, showcasing three distinct states under various mechanical loading conditions.

Methodically considering thermodynamics and Maxwell's Equations, Equation 1 provides the relationship between the generated electric displacement and mechanical strain in a piezoelectric [6].

$$\begin{aligned} D_m &= \varepsilon_{mn}^S E_n + e_{mkl} S_{kl} \\ T_{ij} &= -e_{ijn} E_n + s_{ijkl}^E S_{kl} \end{aligned} \quad (1)$$

Where all the variables and material parameters are defined in Table 1. The superscripts of the material parameters point out which physical quantities are presumed to stay constant in the framework of parameter identification.

Table 1. Expression used in Equation 1.

Notation	Description	Unit
Intensive state variables		
E_n	Electric field density; vector	Vm^{-1}
T_{kl}	Mechanical stress; tensor rank 2	Nm^{-2}
Extensive state variables		
D_m	Electric flux density; vector	Cm^2
S_{ij}	Mechanical strain; tensor rank 2	-
Material parameter		
$\varepsilon_{mn}^{T,\theta}$	Electric permittivity; tensor rank 2	$\text{AsV}^{-1}\text{m}^{-1}; \text{Fm}^{-1}$
e_{mkl}	Piezoelectric stress constants; tensor rank 3	$\text{Cm}^{-2}; \text{NV}^{-1}\text{m}^{-1}$
$s_{ijkl}^{E,\theta}$	Elastic compliance constants; tensor rank 4	m^2N^{-1}

Equation 1 comprises two terms: the first term defines mechanically induced electric charge, which we aim to utilize, while the second term, representing electrically induced stress, will be disregarded. The $\varepsilon_{mn}^S E_n$ term defines the electrical displacement resulting from the application of an electric field and the $e_{mkl} S_{kl}$ term is generated by a mechanical strain. Since there is no external application of an electric field in this study, the former term can also be disregarded. Consequently, the most relevant equation linking mechanical strain to electrical displacement is expressed in Equation 2.

$$D_m = e_{mkl} S_{kl} \quad (2)$$

The next step involves thoroughly studying both the electrical and mechanical models to understand how the piezoelectric strain meter behaves when subjected to mechanical forces.

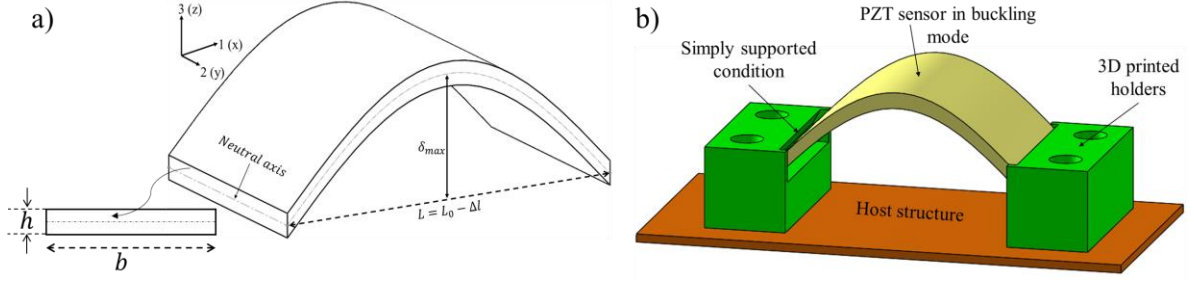


Fig. 2. The schematic of the buckled thin plate a) with simply supported (pinned) boundary condition considering coordinates notation and physical dimensions and b) how to apply the buckling condition using the 3D printed extension (holders) and installation on the host structure.

1.2 Electromechanical model of piezoelectric sensor

Fig. 3. a illustrates a simplified comprehensive model of a piezoelectric sensor, encompassing both resonant and non-resonant components [11], along with a current source based on electrical displacement. Comparatively, the resistance of R_p is much greater than R_s and R_m . Additionally, at resonance, the impedance of L_m and C_m conjugates, resulting in zero overall impedance, with R_m being the dominant impedance across the circuit. However, at lower frequencies, the impedance of the resonant branch surpasses that of other branches, rendering it negligible. Furthermore, at frequencies below 100 Hz, the impedance of capacitor C outweighs that of R_s , allowing R_s to be disregarded. Under these assumptions, the equivalent circuit reduces to parallel R_p and C , alongside I_D as depicted in Fig. 3.b. Additionally, R_L represents the external load resistor, which may stem from measurement equipment or designated electronic circuits [12].

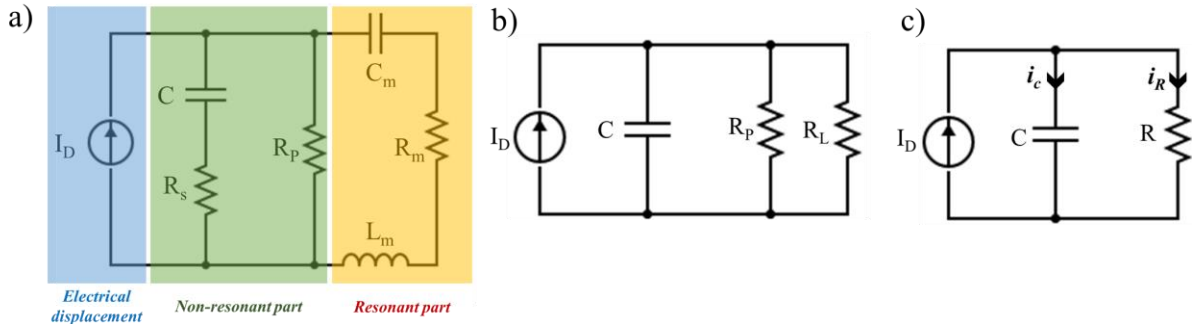


Fig. 3. Equivalent circuit of a piezoelectric sensor a) for a wide range of frequency, b) in a very low frequency range ($f \ll f_r$) including load resistor and c) simplified circuit with an equivalent resistor.

Now there is a first order parallel RC circuit, the capacitor C is simulating inherent capacitance of piezoelectric sensor and is defined by physical dimension and material properties of the sensor. Under assumptions of plane-strain and thin film uniaxial strain, the dielectric permittivity can be defined as an effective term \bar{k} [9] :

$$\bar{\epsilon} = \epsilon_{33} + \frac{e_{33}^2}{c_{33}} \quad (3)$$

where ϵ_{33} is the dielectric permittivity along thin film's normal direction and c_{33} is the elastic constant. Under thin film plane-strain assumption, the transversal strain $s_{22} = 0$ and an effective piezoelectric coefficient can be defined as Equation 4 [13]:

$$\bar{e} = e_{31} - \frac{c_{13}}{c_{33}} e_{33} \quad (4)$$

To convert the electrical displacement from Equation 2 to electrical current, the current density (J) and the whole generated current considering sensor area (A) can be defined by Equation 5.

$$I_D = A \cdot J_D = A \cdot \frac{dD_m(t)}{dt} = A \frac{d\bar{e}S}{dt} = A\bar{e} \frac{dS(t)}{dt} \quad (5)$$

Where $S(t)$ is the uniaxial strain of the bent piezoelectric thin film. Applying Kirchoff's current law to the circuit in Fig. 3.c, Equation 6 describes the current distribution in the circuit.

$$I_D = i_c + i_R = C \frac{dv}{dt} + \frac{v}{R} \quad (6)$$

Equation 6 describes I_D and combined with Kirchoff's law will conduct a first-order differential Equation that relates sensor output voltage (v) to dynamic strain $S(t)$. By considering initial conditions as $v_i = 0$, the generated voltage by piezoelectric can be described by Equation 7:

$$v(t) = \frac{A\bar{e}}{C} e^{-\frac{t}{\tau}} \int_0^t e^{\frac{t}{\tau}} \frac{dS(t)}{dt} dt \quad (7)$$

Where $\tau = RC$ is defined as the time constant of a piezoelectric sensor. This τ also indicates the speed at which the piezoelectric sensor discharges.

To gain insights into the dynamic behaviour of the piezoelectric sensor in buckling mode under the specified boundary conditions—both ends simply supported, as depicted in Fig. 2b—a bending energy approach will be pursued. Considering the use of three different materials in the sensor composition (Fig. 4b), the effective Young's modulus E_{eff} , is defined[13][14]. The strain within the PZT layer (as expressed in Equation 8) exhibits a correlation with the curvature, $w_{(x)}$, of the sensor subsequent to deformation, and is further governed by the moment of inertia, denoted as $M = E_{eff}I_{eff}w''_{(x)}$. Here I_{eff} denotes the effective moment of inertia of the whole sensor.

$$S_{PZT} = \frac{M}{E_{PZT}I_{eff}} \frac{h_{PZT}}{2} = \frac{E_{eff}}{E_{PZT}} \frac{h_{PZT}}{2} w''_{(x)} \quad (8)$$

Furthermore, to assess the strain Equation in dimensional terms, the term $w''_{(x)}$ should possess units of $[\frac{1}{m}]$. The deformation of the sensor $w_{(x)}$ under conditions of simply supported, is given by Equation 9[15]:

$$w_{(x)} = \delta_{max} \sin\left(\frac{\pi}{L}x\right) \quad (9)$$

The length L is defined as $L_0 - \Delta L$ as illustrated in Fig. 2. Where the maximum deflection δ_{max} , is defined by Equation 10:

$$\delta_{max} = \sqrt{\frac{4L_0\Delta L}{\pi^2} - \frac{h_{PZT}^2}{9}} \approx \frac{2}{\pi} \sqrt{L_0\Delta L} \quad (10)$$

The $w_{(x)}$ at the midpoint of the sensor, where the strain is the highest, can be inserted into Equation 8 to give the governing equation for strain. In the experimental setup, the change in length, ΔL varies over time and is modulated by the initial buckling, as depicted in Fig. 4d.

2. Experimental Method

2.1 Material

The piezoelectric sensor utilized in the research is a P-876 soft PZT piezoelectric transducer manufactured by PI company. It employs a PIC255 piezoceramic material, the shape and dimensions of which are illustrated in Fig. 4a. This particular type of soft ceramic possesses the capability of limited bending while maintaining the integrity of its ceramic structure, thereby mitigating the risk of breakage. However, it is noteworthy that this sensor can undergo buckling, with the minimum bending radius specified as 20 mm, as indicated in the sensor datasheet.

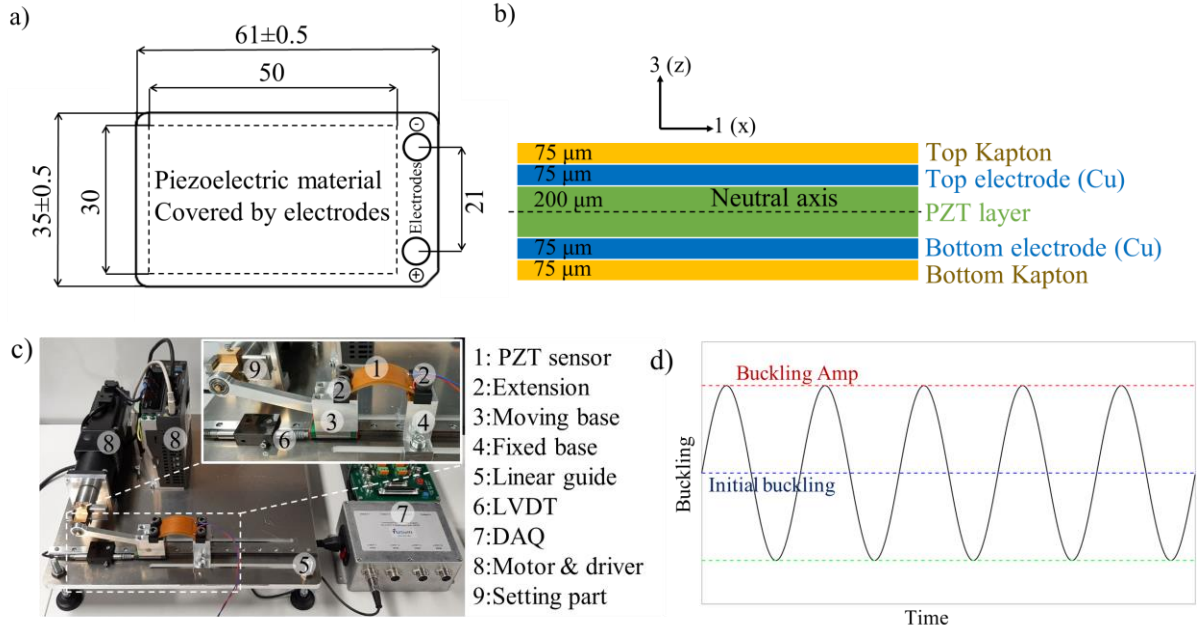


Fig. 4. a) schematic illustrating sensor dimensions, sourced from the P-876 datasheet, b) different layers configuration, c) Illustration of the developed test setup for applying dynamic buckling to the PZT sensor and d) Buckling profile.

2.2 Test method

In this section, the developed equation is evaluated through experimental validation, encompassing three key parameters: initial, and dynamic buckling amplitude, and dynamic buckling frequency. MATLAB is employed for the analytical assessment. Consequently, the initial buckling, while adhering to the assumption $B_{initial} \geq B_{Amp}$, plays a significant role in the distribution of strain within the piezoelectric sensor. To investigate the impact of initial buckling on output voltage, four different ranges (3, 5, 9, and 11 mm) are considered, alongside variations in dynamic buckling and frequency ranging from 1 to 10 Hz. These analyses are presented in Fig. 5a-d for experimental measurements and Fig. 5e-h for analytical results.

3. Results and discussions

In this section, the developed equation is evaluated through experimental validation, encompassing three key parameters: initial, and dynamic buckling amplitude, and dynamic buckling frequency. MATLAB is employed for the analytical assessment. Consequently, the initial buckling, while adhering to the assumption $B_{initial} \geq B_{Amp}$, plays a significant role in the distribution of strain within the piezoelectric sensor. To investigate the impact of initial buckling on output voltage, four different ranges (3, 5, 9, and 11 mm) are considered, alongside variations in dynamic buckling and frequency ranging from 1 to 10 Hz. These analyses are presented in Fig. 5a-d for experimental measurements and Fig. 5e-h for analytical results.

The relationship between buckling amplitude and output voltage is found to be linear, as buckling amplitude directly corresponds to strain amplitude, resulting in a proportional output current. However, frequency, derived from strain, does not follow this linearity. Furthermore, the graphs indicate an optimal initial buckling chord of 9 mm, leading to higher output voltage. Further precise determination of this optimal point requires additional experiments and analytical scrutiny.

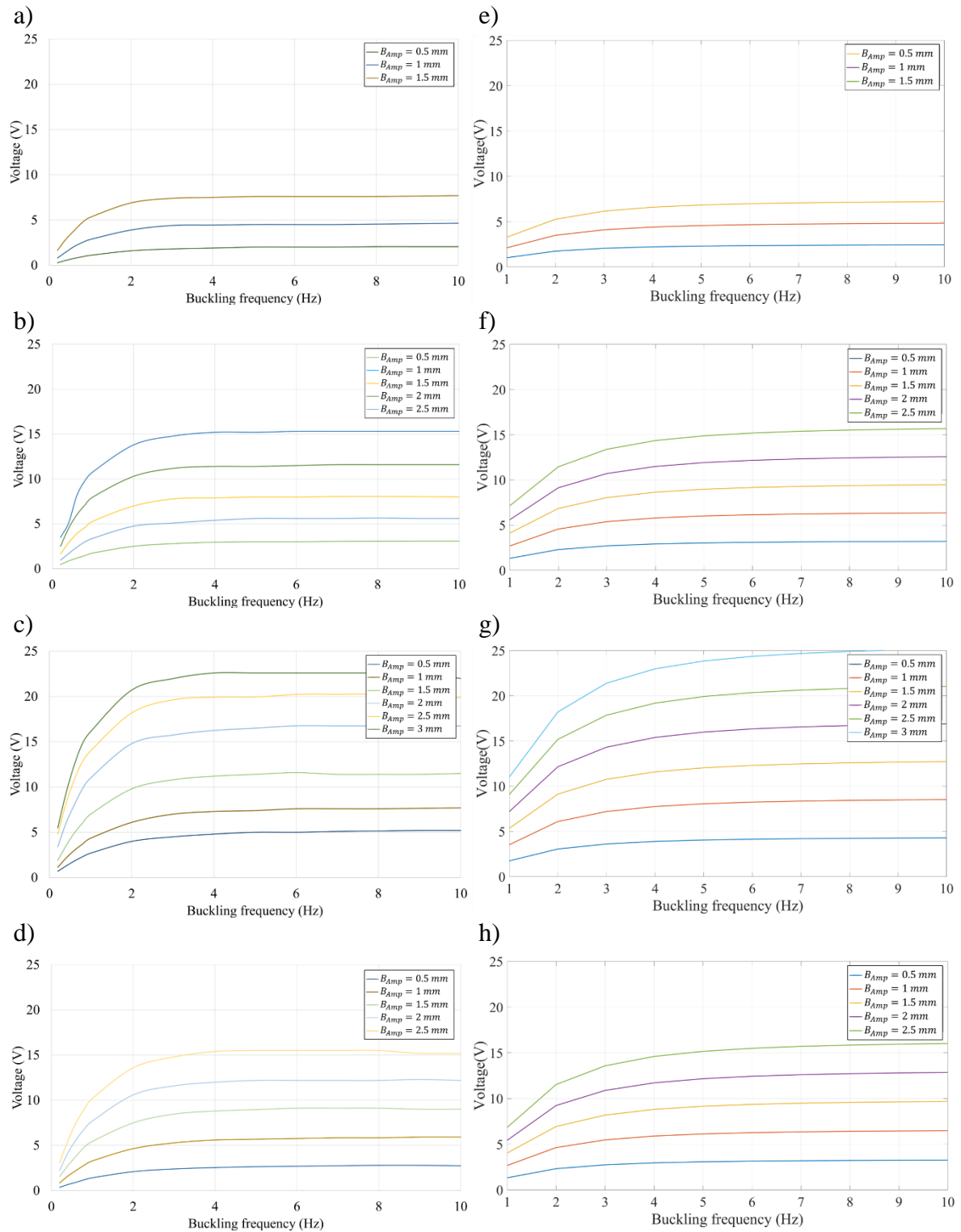


Fig. 5. Experimental measurements of Output Voltage as a Function of Buckling Frequency, Demonstrating Static and Dynamic Buckling within a Frequency Range of 1 to 10 Hz. Initial Buckling Values: a) 3 mm, b) 5 mm, c) 9 mm, and d) 11 mm. Analytical Results of Initial Buckling Values: e) 3 mm, f) 5 mm, g) 9 mm, and h) 11 mm.

3. Conclusions

This study presents an integrated analytical and experimental method for fatigue life monitoring using a soft PZT piezoelectric sensor operating in buckling mode. The main aim was to establish a reliable technique for assessing the fatigue life of engineering structures,

crucial for ensuring their safety and durability. The incorporation of a 3D-printed 'Extension' provided a sturdy platform for the piezoelectric sensor, enabling its operation in buckling mode under cyclic strains. The developed analytical framework established a direct correlation between dynamic strain values and sensor output, considering key attributes like amplitude and strain rate. Experimental validation demonstrated the effectiveness of the proposed approach under various dynamic loading conditions, showcasing the high sensitivity and functionality of the integrated piezoelectric sensor with the 3D-printed extension as a passive dynamic strain measurement sensor. This integration offers notable advantages, including self-powering capabilities and enhanced safety in highly strained structures. Future research should concentrate on refining the approach and expanding its applicability, with a focus on impedance calculations and conducting more precise experiments to understand sensor behaviour in real-world scenarios. Addressing these aspects will contribute to advancing fatigue life monitoring, thereby enhancing the safety and performance of engineering structures globally.

References

- [1] Á. Cunha, E. Caetano, F. Magalhães, and C. Moutinho, 'Dynamic identification and continuous dynamic monitoring of bridges: different applications along bridges life cycle', *Struct. Infrastruct. Eng.*, vol. 14, no. 4, pp. 445–467, Apr. 2018, doi: 10.1080/15732479.2017.1406959.
- [2] 'Fatigue and Durability of Structural Materials - Gary R. Halford - Google Books'.
- [3] N. Noppe, K. Tatsis, E. Chatzi, C. Devriendt, and W. Weijtjens, 'Fatigue stress estimation of offshore wind turbine using a Kalman filter in combination with accelerometers', doi: 10.3929/ethz-b-000346296.
- [4] M. Elsherif *et al.*, 'Optical Fiber Sensors: Working Principle, Applications, and Limitations', *Adv. Photonics Res.*, vol. 3, no. 11, p. 2100371, Nov. 2022, doi: 10.1002/ADPR.202100371.
- [5] S. Duan, J. Wu, J. Xia, and W. Lei, 'Innovation Strategy Selection Facilitates High-Performance Flexible Piezoelectric Sensors', *Sensors 2020, Vol. 20, Page 2820*, vol. 20, no. 10, p. 2820, May 2020, doi: 10.3390/S20102820.
- [6] S. J. Rupitsch, 'Piezoelectric Sensors and Actuators', 2019, doi: 10.1007/978-3-662-57534-5.
- [7] A. Ghaderiaram, R. Mohammadi, E. Schlangen, and M. Fotouhi, 'Development of an Innovative Extension for Fatigue Life Monitoring Using a Piezoelectric Sensor', *Procedia Struct. Integr.*, vol. 52, pp. 570–582, Jan. 2024, doi: 10.1016/J.PROSTR.2023.12.057.
- [8] J. Sirohi and I. Chopra, 'Fundamental Understanding of Piezoelectric Strain Sensors', 2001, doi: 10.1106/8BFB-GC8P-XQ47-YCQ0.
- [9] J. Chen, N. Nabulsi, W. Wang, J. Y. Kim, M. K. Kwon, and J. H. Ryou, 'Output characteristics of thin-film flexible piezoelectric generators: A numerical and experimental investigation', *Appl. Energy*, vol. 255, no. July, p. 113856, 2019, doi: 10.1016/j.apenergy.2019.113856.
- [10] M. Krommer, P. Berik, Y. Vetyukov, and A. Benjeddou, 'Piezoelectric d 15 shear-response-based torsion actuation mechanism: An exact 3D Saint-Venant type solution', *Int. J. Smart Nano Mater.*, vol. 3, no. 2, pp. 82–102, 2012, doi: 10.1080/19475411.2011.649807.
- [11] M. J. Guan and W. H. Liao, 'On the equivalent circuit models of piezoelectric ceramics', *Ferroelectrics*, vol. 386, no. 1, pp. 77–87, 2009, doi: 10.1080/00150190902961439.
- [12] J. Chen, N. Nabulsi, W. Wang, J. Y. Kim, M. K. Kwon, and J. H. Ryou, 'Output characteristics of thin-film flexible piezoelectric generators: A numerical and experimental investigation', *Appl. Energy*, vol. 255, p. 113856, Dec. 2019, doi: 10.1016/J.APENERGY.2019.113856.
- [13] C. Dagdeviren *et al.*, 'Conformal piezoelectric energy harvesting and storage from motions of the heart, lung, and diaphragm', *Proc. Natl. Acad. Sci. U. S. A.*, vol. 111, no. 5, pp. 1927–1932, Feb. 2014, doi: 10.1073/PNAS.1317233111/SUPPL_FILE/SM04.WMV.
- [14] M. Birsan, D. Pietras, and T. Sadowski, 'Determination of effective stiffness properties of multilayered composite beams', *Contin. Mech. Thermodyn.*, vol. 33, no. 4, pp. 1781–1803, Jul. 2021, doi: 10.1007/S00161-021-01006-2/FIGURES/16.
- [15] B. Xu, L. Wang, C. Xiang, and Z. Han, 'Analysis of Buckling Deformation for the Side Plate of Rectangular CSFT Column Based on Plate Theory with Bi-Axial Loads', *Build. 2022, Vol. 12, Page 626*, vol. 12, no. 5, p. 626, May 2022, doi: 10.3390/BUILDINGS12050626.